Flow Turbulence Combust (2009) 83:307–322
DOI 10.1007/s10494-009-9216-0

Direct Computations of Boundary Layers Distorted by Migrating Wakes in a Linear Compressor Cascade

T. A. Zaki · J. G. Wissink · P. A. Durbin · W. Rodi

Received: 16 September 2008 / Accepted: 30 March 2009 / Published online: 21 April 2009

Abstract A Direct Numerical Simulation (DNS) of flow in the V103 Low-Pressure (LP) compressor cascade with incoming wakes was performed. The computational geometry was chosen largely in accordance with the setup of the experiments performed by Hilgenfeld and Pfitzner (J Turbomach 126:493–500, 2004) at the University of the Armed Forces in Munich. The computations were carried out on the NEC-SX8 in Stuttgart using 64 processors and 85 million grid points. The incoming wakes stemmed from a separate DNS of incompressible flow around a circular cylinder with a Reynolds number of $Re_d = 3300$ (based on mean inflow velocity and cylinder diameter). The boundary layer along the suction surface of the blade was found to separate and roll up due to a Kelvin–Helmholtz instability triggered by the periodically passing wakes. Inside the rolls further transition to turbulence was found to occur. The boundary-layer flow along the pressure surface did not separate, instead it underwent by-pass transition.

Keywords Wakes · Separation · Bypass transition · Compressor

T. A. Zaki (✉)
Department of Mechanical Engineering, Imperial College London,
Exhibition Road, SW7 2AZ London, UK
e-mail: t.zaki@imperial.ac.uk

J. G. Wissink
School of Engineering and Design, Brunel University, Uxbridge, UK
e-mail: jan.wissink@brunel.ac.uk

P. A. Durbin
Aerospace Engineering, Iowa State University, Ames, IA 50011, USA
e-mail: durbin@iastate.edu

W. Rodi
Institute for Hydromechanics, University of Karlsruhe, Karlsruhe, Germany
e-mail: rodi@ifh.uka.de

1 Introduction

Recently, periodic unsteady flow in the Low Pressure (LP) turbine stages of turbo-machines has received a great deal of attention, particularly the influence of transition on the aerodynamic performance of LP turbines [2]. The role of transition in compressor stages of turbo-machines is less studied. In comparison to the LP turbine, transition in compressor passages can be promoted by the adverse pressure gradient condition, which also increases the risk of separation. Whether transition of the boundary layer to turbulence can suppress separation can therefore play an important role in compressor performance. Laminar-to-turbulent transition can be triggered by wakes originating from the upstream stages, unstable Tollmien–Schlichting waves, background turbulence, or a combination of these. Zaki et al. [3] have carried out a Direct Numerical Simulation (DNS) of the interaction of grid-generated free-stream turbulence with the boundary layers in a compressor passage. To date, however, no DNS of wake interaction with compressor blade boundary layers has been reported in the literature. Therefore, there is a clear need for detailed quantitative study of the role of impinging wakes in compressor aerodynamics, at transitional Reynolds numbers.

1.1 Simulations of transitional turbomachinery flows

By utilizing high-performance computational resources, it has become feasible to carry out Large-Eddy Simulations (LES) and Direct Numerical Simulations (DNS) of flow around mid-span sections of a linear turbo-machinery cascade. Previous LES of the turbine passage include, for instance, the work of Michelassi et al. [4] and Raverdy et al. [5]. Direct numerical simulations, while computationally more demanding, are still possible at the range of transitional Reynolds numbers. Examples include the DNS by Wu and Durbin [6], Kalitzin et al. [7], and Wissink and co-workers [8–10].

Separation and transition to turbulence are both likely to be promoted by the mean flow deceleration through the compressor. Both phenomena were studied in the context of turbine passages, although in the presence of an overall favorable pressure gradient. Wu and Durbin [6] simulated flow in a T106 cascade with periodically incoming wakes. They observed that the incoming wakes are distorted as they convect through the passage. On the suction surface, turbulent spots are observed near the rear of the blade, in the adverse pressure gradient section of the airfoil. Near the pressure surface, two sets of elongated, streamwise vortices are observed: one near the free-stream and the second inside the boundary layer. Despite their formation on the concave surface of the blade, they are not of the Görtler type. Instead, they are induced by the distorted wakes in the passage. Another DNS of the T106 cascade was carried out by Kalitzin et al. [7]. They replaced the incoming wakes with free-stream turbulent perturbations, with an inlet turbulence intensity of $T_u = 5\%$. Bypass transition on the suction surface of the blade persisted in those simulations and took place at approximately the same streamwise location as in the case of migrating wakes.

Similar simulations of turbine passages were performed, at lower Reynolds numbers and higher angle of attack, by Wissink [8, 10]. In the absence of wakes, separation was observed on the downstream half of the suction side. In the presence

of realistic wakes, separation was periodically suppressed. Numerical experiments were carried out in order to determine the role of the various scales within the wake [10]. By removing the small-scale fluctuations from the inlet wakes, it was found that the time-periodic large-scale movement of the wake, which resembles a negative jet, was sufficient to trigger a Kelvin–Helmholtz instability of the separated boundary layer. Owing to the absence of small-scale fluctuations, transition to turbulence inside the rolls of recirculating flow was not observed and no kinetic energy was produced at the apex of the deformed wakes.

1.2 The influence of adverse pressure gradient

Typical Reynolds numbers of flows in LP compressors are similar to the Reynolds numbers of flows in LP turbines. In the latter, the overall favorable pressure gradient and the presence of free-stream fluctuations, together, are sufficient to completely suppress boundary-layer separation. In the compressor, the behavior of the boundary layers is more complex: The adverse pressure gradient can cause boundary layer separation. It does, however, also enhance the growth rate of Tollmien-Schlichting (TS) waves and, as a result, can cause early transition. Indeed Hughes and Walker [11] observed growth of discrete instability waves upstream of transition in a compressor case. Additionally, the free-stream turbulence and wakes can alter the breakdown of TS waves. At high intensities, they can completely bypass the discrete instability modes and cause bypass transition [12, 13].

Fundamental studies of these interactions have appeared in the literature. For instance, Zaki and Durbin [14] studied the influence of pressure gradients on boundary layer streaks and breakdown in the framework of continuous mode transition [15]. They observed that adverse pressure gradient enhances the amplification of streaks and, as a result, their secondary instability and breakdown to turbulence. The interaction of streaks with Tollmien–Schlichting waves was studied by Liu et al. [16]. They noted that the streaks reduce the amplification of TS waves, but can lead to a secondary instability, which can be related to the streak spanwise wavelength. The secondary instability is followed by breakdown to turbulence. These fundamental studies were carried out in simple geometric settings. In the compressor, the influence of the leading edge, the curvature of the blade surface, and pressure gradient are all included.

In laboratory experiments, Hilgenfeld and Pfitzner [1] studied the effects of both incoming wakes and grid turbulence on the separating boundary layer flow of a compressor passage (the blade designation in their experiments is V103). The grid turbulence that was generated in the inflow plane was found to obscure the added influence of the periodically incoming wakes on the boundary layer transition. Therefore, in the first DNS of flow in the V103 compressor passage at a Reynolds number of $Re = 138\,500$ (based on mean inflow velocity and the axial chord length), we focused on the effect of free-stream turbulence alone on the separated boundary-layer flow (see Zaki et al. [3]). In the presence of moderate levels of free-stream turbulence, $T_u \sim 3\%$, only the boundary layer along the suction side was found to separate, while without free-stream turbulence the boundary layer was found to separate along both sides of the blade. In the present DNS, we study the influence of the periodically impinging wakes alone and their interaction with the separated boundary layers along the V103 compressor blades.

The angle of attack in the experiments could not be measured reliably. The simulations were therefore performed at the design angle of attack. Given the sensitivity of the flow to this parameter, the pressure distribution from the DNS and the experiments were not in quantitative agreement. However, key features of the mean flow, in particular boundary layer separation and transition to turbulence, were consistent between the numerical and physical experiments.

2 Computational Details

The three-dimensional, incompressible Navier–Stokes equations were discretised using a finite-volume method with a collocated variable arrangement. The spatial discretization scheme was centered, and second-order accurate. Momentum interpolation was employed in order to avoid decoupling of the pressure and the velocity fields, and the Poisson equation for the pressure was solved using the strongly implicit procedure (SIP). The time integration of the system was carried out using a three-stage Runge–Kutta algorithm.

Figure 1 (upper part) shows a spanwise cross-section through the computational domain. The Reynolds number, $Re = 138\,500$, was based on the mean inflow velocity U_0 and the axial chord-length L. At the surface of the blades a no-slip boundary condition was prescribed and at the outlet a convective outflow boundary condition was used. Periodicity was enforced in the spanwise direction and in the vertical direction, both upstream and downstream of the blades. The spanwise size of the computational domain was $l_z = 0.15L$ and the pitch, P, between blades was $P = 0.5953L$.

A cross-section of the computational grid is shown in the lower part of Fig. 1; every eighth grid-line is plotted. The number of grid points in the streamwise, wall-normal, and spanwise directions was $1030 \times 640 \times 128$ points respectively, and their distribution is determined by the elliptic mesh generation algorithm of Hsu and Lee [17]. The refinement of the mesh was based on experience gained previously in performing various DNS of flow in LP turbine cascades. In addition, a preliminary coarse

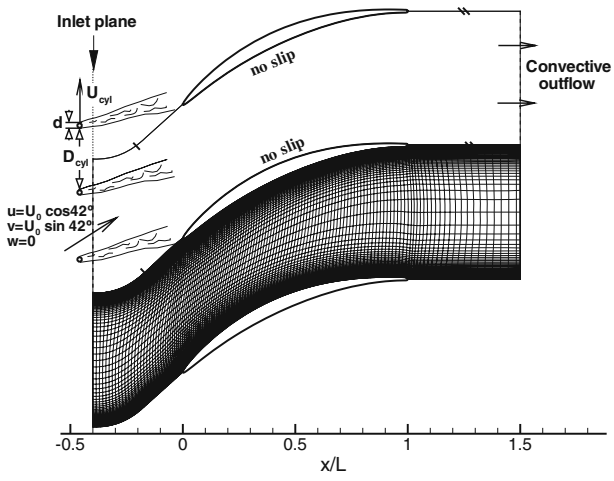

Fig. 1 Side view of the computational domain

grid simulation of the compressor passage was performed in order to identify the grid requirement for resolving both the suction and the pressure surface boundary layers, and any thin separation regions. The code was parallelised using the standard Message Passing Interface (MPI) protocol.

The setup of the DNS is largely based on the laboratory experiment of Hilgenfeld and Pfitzner [1]. The wakes were introduced at the inflow plane, located at $x/L = -0.4$, with a vertical separation of $D = 0.5P$. The half-width of the wakes was $b \approx 0.025L$ and the mean velocity deficit was approximately $0.14U_0$. The wakes moved vertically upwards with a velocity of $U_{cyl} = 0.30U_0$. Hence, the time needed for one wake-passing period was $T = 0.9922L/U_0$. The wakes were generated using a separate DNS of flow around a circular cylinder [18]. The cylinder simulation was at $Re_d = 3300$, where Re_d was based on the cylinder diameter d and the free-stream velocity of the oncoming, uniform flow. From that simulation, a time sequence of 1057 snapshots of the instantaneous field in a vertical plane six diameters downstream of the cylinder was stored, and processed to generate the inflow perturbation for the DNS of the compressor passage. The series of snapshots covered 12 vortex-shedding cycles and was chosen such that the phase of the first snapshot was the same as the phase of the $1057+1^{th}$ snapshot. To transfer the series of snapshots $\left(s_{y,z}^{(k)}\right)|_{k=1}^{1057}$ into a well-behaved periodic signal $\left(\hat{s}_{y,z}^{(k)}\right)|_{k=1}^{1057}$ a Gaussian-like filter $w_i^{(k)}$ was applied:

$$\hat{s}_{y,z}^{(k)} = \sum_{i=-5}^{5} \left\{ w_i^{(k)} s_{y,z}^{[mod(k-i-1,1057)+1]} \right\},$$

where $k = 1, \ldots, 1057$. The filter weights were given by

$$w_i^{(k)} = \lambda_k \ \exp\left(\frac{-i^2}{2\sigma_k^2}\right), \tag{1}$$

where $i = -5, \ldots, 5,$, $k = 1, \ldots, 1057$, λ_k is a factor used to normalise (1), i.e.

$$\lambda_k = \frac{1}{\sum_{j=-5}^{5} \left\{ w_j^{(k)} \right\}},$$

and σ_k is defined by

$$\sigma_k = \frac{5}{\sqrt{min(k, 1058-k)}}, \ k = 1, \ldots, 1057.$$

Figure 2 shows the weights $w_i^{(k)}$ of the filter for various values of k and illustrates that the filter was designed such that it only significantly alters the snapshots in the first and last period of the series in order to get a smooth transition from $\left(\hat{s}_{y,z}^{(1057)}\right)$ to $\left(\hat{s}_{y,z}^{(1)}\right)$. By employing the periodicity of the filtered series $\hat{s}^{(k)}$, an "endless" series of snapshots was obtained.

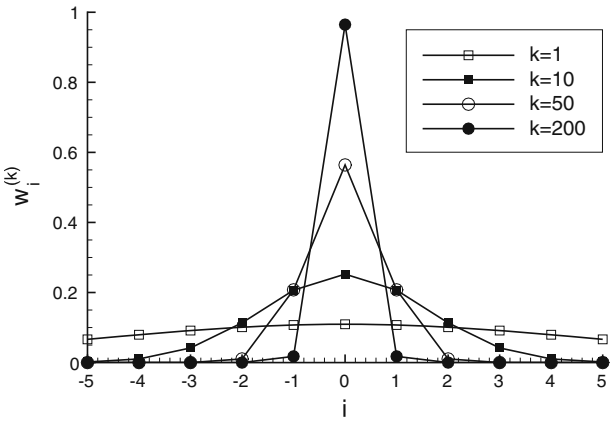

Fig. 2 Filter weights $w_i^{(k)}$ for $k = 1, 10, 50, 200$

3 Results

The flow through the compressor passage was simulated for ten wake-passing periods in order to compute statistical averages. Both the time average, denoted by an overbar, and the phase average, denoted $\langle\cdot\rangle$, are used in the following discussion. The latter is obtained by averaging flow quantities at a particular phase, ϕ, of the wake-passing period,

$$\langle f\rangle(\phi) = \frac{1}{N}\sum_{n=1}^{N} f\,(t = \phi T + nT)\,.$$

As a result, the convergence of phase-averages is challenging, and requires a very large sample size. Instantaneous flow quantities will be decomposed into a mean and fluctuating components according to,

$$f = \bar{f} + \hat{f}(\phi) + f'(\phi) = \langle f\rangle(\phi) + f'(\phi),$$

where $\hat{f}$ is the periodic perturbation to the time-average, and f' is the random fluctuation.

3.1 Averaged quantities

The time-averaged static pressure distribution along the compressor blade is shown in Fig. 3, where

$$C_p \equiv \frac{\bar{p} - \bar{p}_{ref}}{\frac{1}{2}\rho U_{ref}^2}.$$

The angle of attack was selected in alignment with the airfoil in order to minimize the stagnation pressure spike near the leading edge. The C_p distribution is reported immediately downstream of the stagnation region. The figure compares the simulation with incoming wakes (solid line) to a base-line computation of the flow through the passage in the absence of any inlet or free-stream disturbances (dashed line). Immediately downstream of the leading edge, the C_p distributions in both

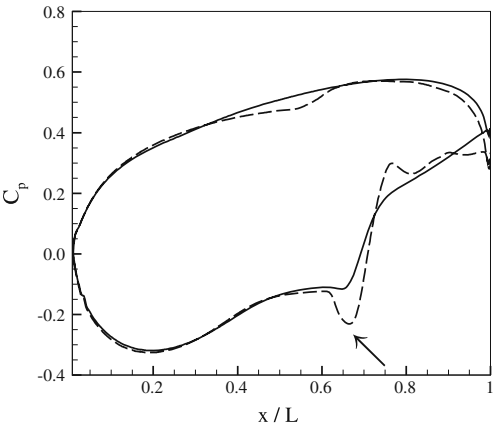

Fig. 3 Mean wall static-pressure in the wake simulation (*solid line*) versus the laminar simulation (*broken line*)

simulations are found to be in good agreement. Farther downstream some differences can be observed: Along the pressure surface (upper curves), the streamwise pressure-gradient is adverse over the interval $0 \leq x/L \leq 0.8$. In the base-line simulation, a distinct kink near $x/L = 0.55$ is observed. This kink, which indicates a possible separation of the pressure side boundary-layer, is absent when the perturbation wakes are introduced.

Along the suction surface (lower curves), differences between the two simulations can be seen in the adverse pressure gradient region downstream of $x/L = 0.2$. Both simulations show a kink in the C_p curve near $x/L \approx 0.67$—identified by the arrow—which is an indication for boundary-layer separation. The fact that the kink in the base-line simulation is considerably more pronounced than in the case with incoming wakes suggests the presence of a much stronger region of reverse flow.

In the region $x/L > 0.8$ of the suction surface (lower curves), the C_p of the base-line simulation indicates that the flow does not fully reattach downstream of the primary separation bubble. In the absence of free-stream perturbations (turbulent wakes or free-stream turbulence), the Kelvin–Helmholtz (KH) rolls which are shed from the separated shear layer do not break up to turbulence causing reattachment, nor do they convect away from the surface giving way to a new attached boundary layer. Instead, they remain coherent and, as they convect downstream, maintain a small patch of reverse flow on the blade surface beneath them. This patch resembles a small separation bubble and moves downstream at the same speed as the Kelvin–Helmholtz rolls. When time-averaged, the small bubbles cause the flat region in the C_p curve of the disturbance-free simulation, for $x/L > 0.8$. In the wake simulation, these small separation bubbles are absent leading to the observed differences in the suction surface C_p distribution among the two simulations.

The phase-averaged kinetic energy of the fluctuations is shown in Fig. 4, at four phases, $\phi = \{0, 0.25, 0.50, 0.75\}$. These phases will be used in subsequent discussions of the influence of the passing wake on the state of the boundary layer on both the pressure and suction surfaces of the blade. The path of the wakes is easily identified in the figure by the local increase in the fluctuating kinetic-energy level in the free stream. Compared to the simulations of flow in the T106 turbine cascade, where the wakes were subjected to severe straining and stretching by the mean flow, in the

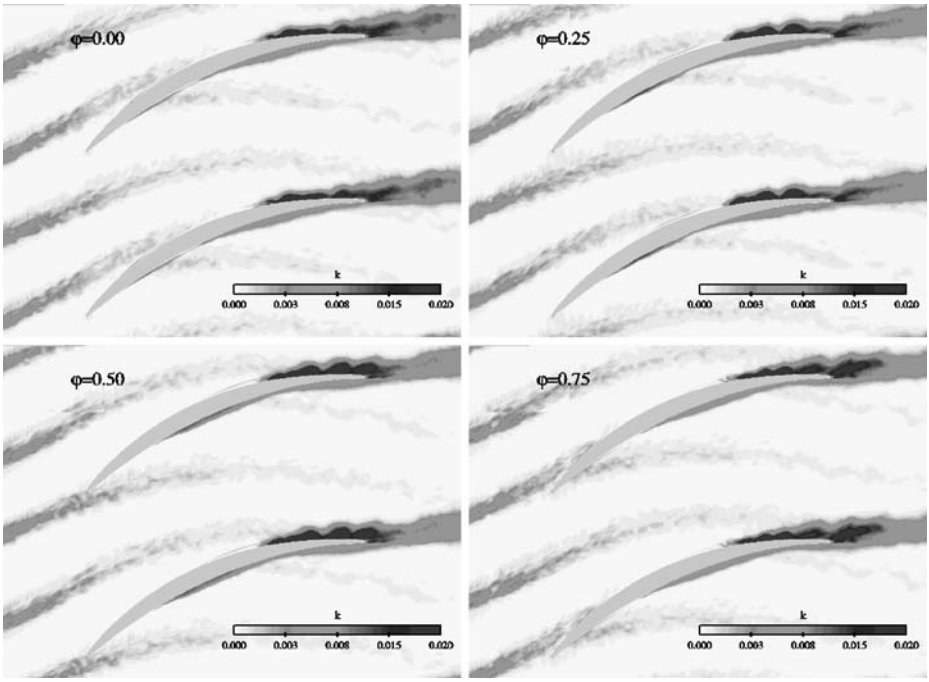

Fig. 4 Contours of the phase-averaged kinetic energy of the fluctuations at four phases $\phi = 0$, 0.25, 0.50, 0.75

compressor cascade the stretching and straining action of the mean flow on the wakes is not significant. Consequently, no production of kinetic energy in the free-stream part of the passage between blades is visible in the figures.

3.1.1 The suction surface

Contours of the phase-averaged spanwise vorticity in the downstream half of the blade are shown in Fig. 5, at the four phases $\phi = \{0, 0.25, 0.50, 0.75\}$. Along the suction side, the separated boundary layer can be seen to roll-up due to a Kelvin–Helmholtz (KH) instability that is periodically triggered by the passing wake. The relative position of the passing wake in each of the phases can be obtained from Fig. 4. A comparison of Figs. 4 and 5 shows that the high production of kinetic energy in the former takes place mostly inside the Kelvin-Helmholtz rolls (see also Wissink [8]).

The coherence of the KH rolls in Fig. 5 is most pronounced at $\phi = 0$ and $\phi = 0.25$. At $\phi = 0$ the separated shear-layer is rolling up and three clearly defined rolls of recirculating flow (labelled I, II and III) can be seen. As the rolls are convected downstream, they are gradually destroyed by the turbulence generated inside them. As a result, the most downstream roll III is slightly more diffuse than the rolls I and II. At $\phi = 0.25$, clearly defined rolls are still shed from the separated shear layer. The location of the shedding has, however, moved slightly downstream. At $\phi = 0.50$ and $\phi = 0.75$ the location where the shear layer disintegrates has moved even further

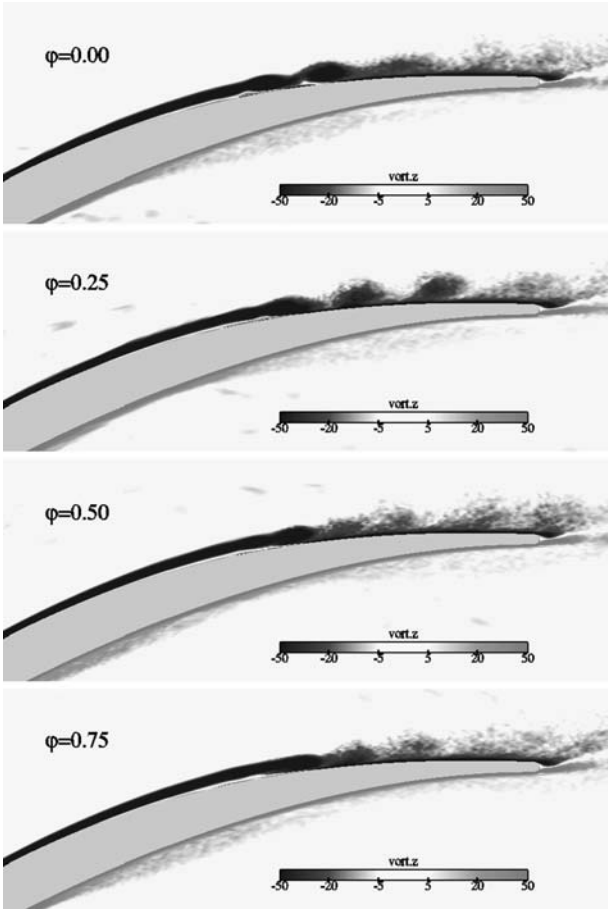

Fig. 5 Contours of the phase-averaged spanwise vorticity at four phases $\phi = \{0, 0.25, 0.50, 0.75\}$

downstream and a wake is impinging on top of the rolls of recirculating flow (see Fig. 4). The small-scale fluctuations in the impinging wake promote a quick transition to turbulence inside the K-H rolls, which explains why the vorticity in the rolls at these phases is rather diffused.

The time and phase averaged skin friction coefficient along the suction surface of the blade are contrasted in Fig. 6. The upper pane of the figure (dashed line) shows the laminar C_f, in the absence of the wakes. The separation location is marked on the figure, at approximately $x/L \approx 0.44$. Laminar reattachment takes place at $x/L \approx 0.77$. Another small region of negative C_f is seen near the trailing edge, at $x/L \approx 0.95$, and is due to the time-average of the convected separation bubbles which shadow the shed laminar K-H rolls. In the presence of wakes (solid line), only the first separation region near $x/L \approx 0.45$ is observed in the time-averaged results.

The four lower panes of Fig. 6 show the phase-avaraged C_f at $\phi = \{0, 0.25, 0.50, 0.75\}$. The separation location, identified by the vertical dashed line, can be seen to alternately move upstream at $\phi = \{0, 0.75\}$, and downstream at $\phi = \{0.25, 0.50\}$. The downstream movement of the separation point at $\phi = \{0.25\}$ is correlated with the interaction of the passing wake with the separated shear layer (see Fig. 4). This

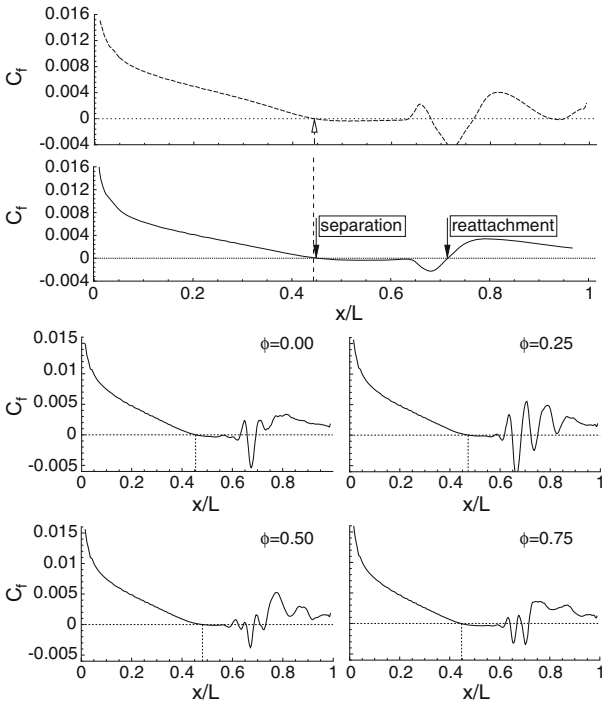

Fig. 6 Friction coefficient along the suction surface of the blade. *Upper panes*: time-averaged C_f (uppermost without wakes, other with wakes); *lower panes*: phase-averaged C_f at four phases of the wake-passing frequency

delay in separation persists until $\phi = \{0.5\}$ when the wake induces the initial stages of breakdown of the K-H rolls into turbulence (Figs. 4 and 5). Beyond this point, for $\phi \in [0.75, 0]$, the wake has convected past the separated shear layer and the separation region relaxes towards a laminar solution. Therefore, separation moves upstream in those phases when the K-H rolls are in the early, near-laminar development stage (see $\phi = \{0.75, 0\}$ of Fig. 5).

The phase averaged separation location along the suction surface is plotted in Fig. 7. The separation point only shows a weak dependence on the phase, in that it alternately moves between $x/L \approx 0.425$ and $x/L \approx 0.445$.

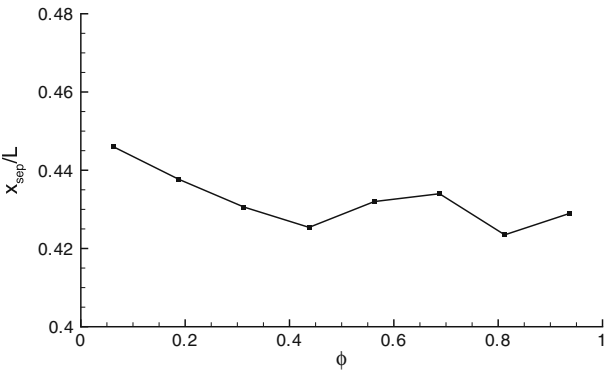

Fig. 7 Phase-averaged separation-location x_{sep} along the suction surface

3.1.2 The pressure surface

It was noted from the time-averaged C_p (Fig. 3) that a mild separation region develops on the pressure surface of the blade in the base-line, disturbance-free simulation. Separation is, however, absent when the passing wakes are introduced. Based on the phase-averaged turbulent kinetic energy (Fig. 4), the impinging wakes manage to locally trigger fluctuations inside the pressure surface boundary-layer, in the adverse pressure-gradient region. These fluctuations are subsequently convected downstream, and they play a significant role in maintaining an attached flow on the pressure surface, throughout the chord of the bade. This role is further explored in this section.

Figure 8 shows the mean friction-coefficient, C_f, along the pressure surface. The laminar C_f distribution (without incoming wakes) is shown in the top-most pane (dashed line). The laminar separation point is identified at $x/L \approx 0.35$, which agrees with the loss of pressure gradient seen in the C_p distribution along the pressure surface in Fig. 3. The region of maximum reverse flow, $x/L \sim 0.55$, also agrees with the kink in the C_p profile. The time-averaged C_f for the passing-wake simulation is also included (solid line). Despite the adverse pressure gradient along a significant portion of the pressure surface, $0 < x/L < 0.8$, the skin friction remains strictly positive when the wakes are introduced. Transition to turbulence is observed at $x/L \approx 0.22$, upstream of the laminar separation point. Downstream, at $x/L \approx 0.8$, C_f rises sharply. This correspond to the turbulent boundary layer being subject to the favorable pressure gradient near the trailing edge (see Fig. 3).

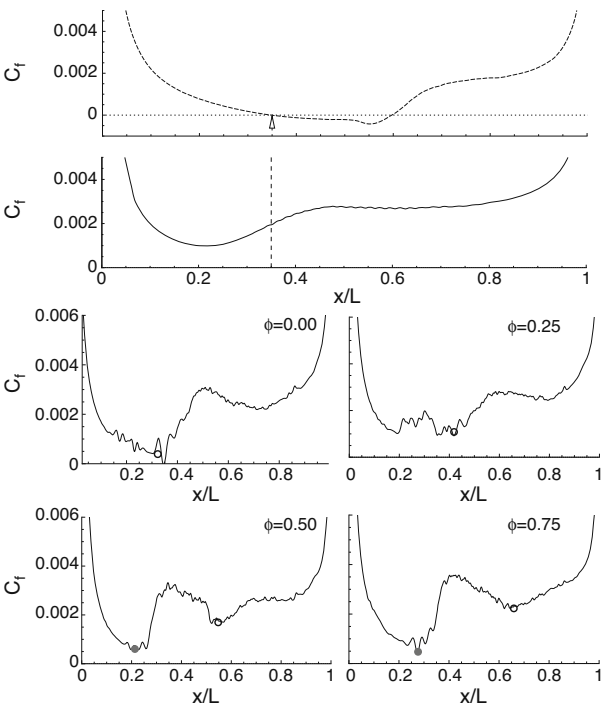

Fig. 8 Friction coefficient along the pressure surface of the blade. *Upper panes*: time-averaged C_f (uppermost without wakes, other with wakes); *lower panes*: phase-averaged C_f at four phases of the wake-passing frequency

The phase-averaged C_f is shown in the lower four panes of Fig. 8 for $\phi = \{0, 0.25, 0.50, 0.75\}$. The open circles identify the onset of a transition event at $\phi = 0$. This point convects downstream in subsequent phases. At $\phi = 0.25$ an emergent instability trails the transition point, and becomes fully turbulent at $\phi = 0.5$. As the boundary layer begins to relax towards the laminar solution, which in the absence of wakes is separated, it is again destabilized by the passing wake. The new transition event at $\phi = 0.5$ is marked in the figure by a filled circle. The short period between two consecutive wakes therefore ensure that the pressure side boundary layer remains attached.

3.2 Instantaneous flow features

In order to identify the mechanism of boundary layer transition to turbulence, we inspect the instantaneous velocity perturbations near the blade surface. Figure 9 shows one such snapshot of the tangential velocity perturbations in two planes, parallel to the pressure (upper part) and suction (lower part) surfaces of the blade. Along the suction surface, the wakes do not, on average or instantaneously, eliminate separation. Instead, a predominantly two-dimensional roll-up due to a Kelvin-Helmholtz (KH) instability is observed, and the KH billows are destabilized and breakdown to turbulence due to high-frequency forcing by the passing wakes. On the other hand, the fluctuations introduced into the pressure surface boundary layer by the impinging wakes manage to completely suppress separation along this side of the blade. The tangential fluctuations show a region of high-amplitude elongated disturbances, or Klebanoff streaks. The streaks are intermittent, and their appearance is correlated with the passing of the wake.

The series of snapshots of the fluctuating streamwise (u') and spanwise (w') velocities shown in Fig. 10 is recorded in a plane close to the pressure surface of the blade. The snapshots are selected to span one wake-passing period. As the

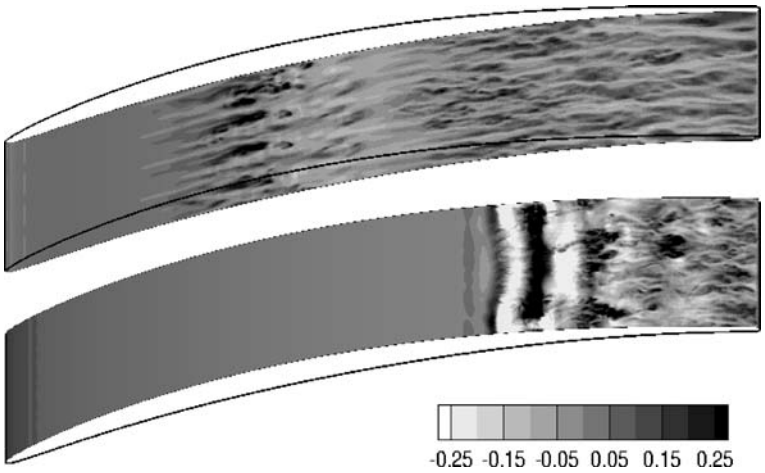

Fig. 9 Snapshot of tangential velocity fluctuations in planes parallel to the pressure (*upper pane*) and the suction surfaces (*lower pane*)

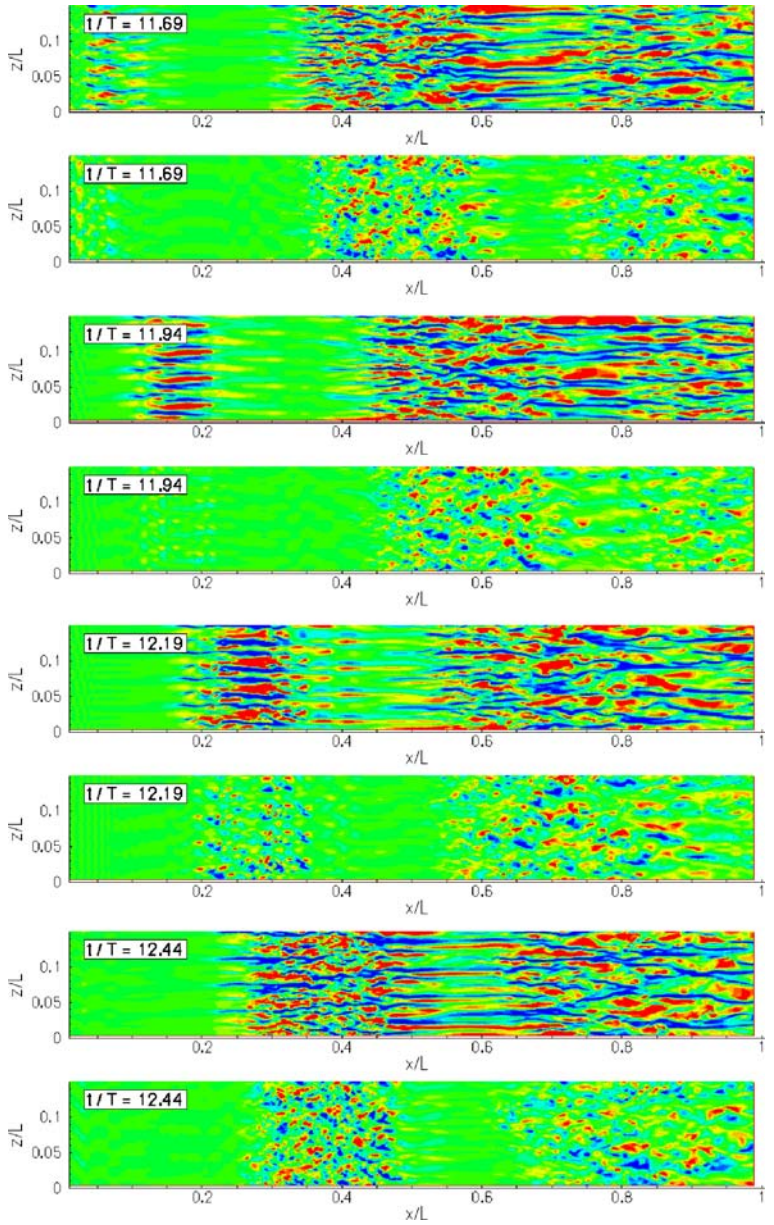

Fig. 10 Snapshots of the fluctuating streamwise velocity u' (*upper part of panes*) and spanwise velocity w' (*lower part of panes*) at $t/T = 11.69, 11.94, 12.19$ and 12.44 in a plane at a distance of $0.0022L$ to the pressure surface of the blade

wake sweeps along the pressure surface of the blade, it triggers disturbances locally inside the boundary layer. The time sequence of Fig. 10 shows that the disturbances convect downstream; they shadow the passing wake, but at a lower speed than the free-stream.

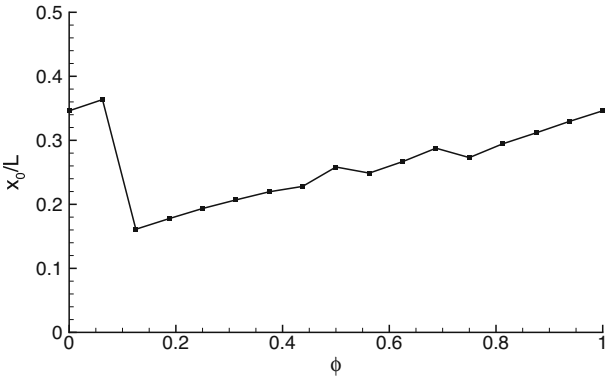

Fig. 11 Phase-averaged location of the onset of transition x_0 along the pressure surface

In the first two time instances of Fig. 10, the wake-induced disturbances are visible at $x/L = 0.05$ and $x/L = 0.18$ respectively. These disturbances are only captured in contours of the streamwise velocity perturbation, which is amplified due to the *lift-up* mechanism: vertical displacement of fluid parcels towards the wall results in a positive u-perturbation; conversely, upward displacement of fluid parcels away from the wall causes a negative u-disturbance. Unlike u' which is amplified, both v' and w' remain on the order of the background turbulence intensity. These elongated disturbances are known as Klebanoff streaks, and are not yet turbulent. The absence of turbulence at these locations is illustrated in the corresponding snapshots of w' shown in the lower frames of each pane.

As the streaks are convected downstream, they become unstable and spanwise fluctuations are found to grow, which is captured in the snapshots at $t/T = 12.19$ around $x/L = 0.28$ and $t/T = 12.44$ around $x/L = 0.40$. The snapshot of w' at $t/T = 12.44$ clearly shows two patches of turbulent flow around $x/L = 0.40$ and $x/L = 0.80$ that were triggered by two wakes that successively impinged on the pressure surface. The patches are separated by a region of becalmed flow that, as shown in the snapshot of u' at $t/T = 12.44$, still contains perturbation streaks.

The instantaneous visualizations of Fig. 10 show that transition location moves upstream and downstream, as a function of phase of the passing wake. Transition onset, which was identified by the minimum in the phase-averaged C_f curve, is shown in Fig. 11 as a function of phase ϕ. At $\phi = 0.125$ the onset of transition is located farthest upstream (at $x/L \approx 0.16$). At smaller x/L, the disturbances introduced into the boundary layer by the periodically impinging wakes do not manage to trigger transition to turbulence. With time (or, equivalently, with increasing phase) transition location is found to move downstream as the disturbances are convected in the boundary layer. The convection speed of the transition point, v_t, is found to be virtually constant, with $v_t \approx 0.2L/T$. It is nearly one third the free-stream convection speed of the wake, $v_w \approx 0.6L/T$.

4 Conclusions

A three-dimensional direct numerical simulation of flow in a linear, low-pressure compressor cascade with periodically passing wakes has been performed. The

impinging wakes were generated in a separate simulation of flow along a circular cylinder at $Re_d = 3300$. The wakes, travelling through the passage between blades, were observed to only slightly alter their trajectory due to the straining and stretching action by the mean flow.

Along the suction side, the boundary layer flow was observed to separate. Transition was subsequently triggered due to the influence of the periodically passing wakes. In the first stage of transition, the separated boundary layer was observed to roll up due to a Kelvin–Helmholtz instability. Inside the rolls, kinetic energy is produced, resulting in a turbulent, wake-like flow adjacent to the surface of the blade downstream of the separation bubble. The location of separation was found to be only weakly phase-dependent.

Along the pressure side, the boundary layer was observed to remain attached for all phases. As the wakes impinge on the adverse-pressure gradient portion of the pressure surface, fluctuations were introduced in the boundary-layer flow, in the shadow of the wake. These fluctuations initially triggered longitudinal structures, or streaks, which became unstable as they were convected downstream. The resulting patches of turbulent flow were separated by a becalmed region (in which streaks were still present). Once the patches of turbulent flow entered the favorable pressure-gradient region, the turbulent fluctuations were largely damped. These turbulent patches, nonetheless, completely suppressed separation along the pressure surface at all phases.

Acknowledgements The authors would like to thank the German Research Foundation (DFG) for funding this research and the steering committee of the Computing Centre in Stuttgart (HLRS) for providing computing time on the NEC SX-8.

References

1. Hilgenfeld, L., Pfitzner, M.: Unsteady boundary layer developement due to wake passing effects on a highly loaded linear compressor cascade. J. Turbomach. **126**, 493–500 (2004)
2. Hodson, H.P., Howell, R.J.: Bladerow interactions, transition, and high-lift aerofoils in low-pressure turbines. Annu. Rev. Fluid Mech. **37**, 71–98 (2007)
3. Zaki, T.A., Durbin, P.A., Wissink, J.G., Rodi, W.: Direct numerical simulation of bypass and wake-induced transition in a linear compressor cascade. In: ASME Turbo Expo, Barcelona, GT2006-90885, 8–11 May 2006
4. Michelassi, V., Wissink, J.G., Fröhlich, J., Rodi, W.: Large-eddy simulation of flow around a low-pressure turbine blade with incoming wakes. AIAA J. **41**, 2143–2156 (2003)
5. Raverdy, B., Mary, I., Sagaut, P., Liamis, N.: High-resolution large-eddy simulation of flow around low-pressure turbine blade. AIAA J. **41**, 390–398 (2003)
6. Wu, X., Durbin, P.A.: Evidence of longitudinal vortices evolved from distorted wakes in a turbine passage. J. Fluid Mech. **446**, 199–228 (2001)
7. Kalitzin, G., Wu, X., Durbin, P.A.: DNS of fully turbulent flow in a LPT passage. In: Rodi, W., Fueyo, N. (eds.) Proceedings of the 5th International Symposium on Engineering Turbulence Modelling and Experiments, Mallorca, Spain, pp. 741–750. Elsevier, Amsterdam (2002)
8. Wissink, J.G.: DNS of separating, low-Reynolds number flow in a turbine cascade with incoming wakes. Int. J. Heat Fluid Flow **24**, 626–635 (2003)
9. Wissink, J.G., Rodi, W.: Direct numerical simulation of flow and heat transfer in a turbine cascade with incoming wakes. J. Fluid Mech. **569**, 209–247 (2006)
10. Wissink, J.G., Rodi, W., Hodson, H.P.: The influence of disturbances carried by periodically incoming wakes on the separating flow around a turbine blade. Int. J. Heat Fluid Flow **27**, 721–729 (2006)

11. Hughes, J.D., Walker, G.J.: Natural transition phenomena on an axial flow compressor blade. J. Turbomach. **123**, 392–401 (2001)
12. Jacobs, R.G., Durbin, P.A.: Simulations of bypass transition. J. Fluid Mech. **428**, 185–212 (2001)
13. Wu, X., Jacobs, R.G., Hunt, J.C.R., Durbin, P.A.: Simulation of boundary layer transition induced by periodically passing wakes. J. Fluid Mech. **398**, 109–153 (1999)
14. Zaki, T.A., Durbin, P.A.: Continuous mode transition and the effects of pressure gradient. J. Fluid Mech. **563**, 357–388 (2006)
15. Zaki, T.A., Durbin, P.A.: Mode interaction and the bypass route to transition. J. Fluid Mech. **531**, 85–111 (2005)
16. Liu, Y., Zaki, T.A., Durbin, P.A.: Boundary layer transition by interaction of discrete and continuous modes. J. Fluid Mech. **604**, 199–233 (2008)
17. Hsu, K., Lee, L.: A numerical technique for two-dimensional grid generation with grid control at the boundaries. J. Comput. Phys. **96**, 451–469 (1991)
18. Wissink, J.G., Rodi, W.: Numerical study of the near wake of a circular cylinder. Int. J. Heat Fluid Flow **29**, 1060–1070 (2008)